

NIH RELAIS Document Delivery

NIH-10289408

JEFFDUYN

NIH -- W1 J0579N

JOZEF DUYN
10 Center Dirve
Bldg. 10/Rm.1L07
Bethesda, MD 20892-1150

ATTN: SUBMITTED: 2002-09-04 08:27:56
PHONE: 301-594-7305 PRINTED: 2002-09-06 14:13:52
FAX: - REQUEST NO.:NIH-10289408
E-MAIL: SENT VIA: LOAN DOC
7999125

NIH Fiche to Paper Journal

TITLE: JOURNAL OF CEREBRAL BLOOD FLOW AND METABOLISM : OFFICIAL
 JOURNAL OF THE INTERNATIONAL SOCIETY OF CEREBRAL BLOOD
 FLOW AND METABOLISM
PUBLISHER/PLACE: Raven Press New York Ny
VOLUME/ISSUE/PAGES:1992 Sep;12(5):734-44 734-44
DATE: 1992
AUTHOR OF ARTICLE: Hugg JW; Duijn JH; Matson GB; Maudsley AA; Tsuruda JS;
 Gelin
TITLE OF ARTICLE: Elevated lactate and alkalosis in chronic human br
ISSN: 0271-678X
OTHER NOS/LETTERS: Library reports holding volume or year
 8112566
 1506441
SOURCE: PubMed
CALL NUMBER: W1 J0579N
REQUESTER INFO: JEFFDUYN
DELIVERY: E-mail: jhd@helix.nih.gov
REPLY: Mail:

NOTICE: THIS MATERIAL MAY BE PROTECTED BY COPYRIGHT LAW (TITLE 17, U.S.
CODE)

----National-Institutes-of-Health,-Bethesda,-MD-----

Elevated Lactate and Alkalosis in Chronic Human Brain Infarction Observed by ^1H and ^{31}P MR Spectroscopic Imaging

*†James W. Hugg, *†Jeff H. Duijn, *‡Gerald B. Matson, *†Andrew A. Maudsley, †Jay S. Tsuruda, †Deborah F. Gelinas, and *†§Michael W. Weiner

*MR Unit, Department of Veterans Affairs Medical Center, San Francisco CA; Departments of †Radiology, ‡Pharmaceutical Chemistry, and §Medicine, University of California, San Francisco CA; †Letterman Army Hospital, San Francisco, CA, U.S.A.

Summary: The goal of this study was to investigate lactate and pH distributions in subacutely and chronically infarcted human brains. Magnetic resonance spectroscopic imaging (MRSI) was used to map spatial distributions of ^1H and ^{31}P metabolites in 11 nonhemorrhagic subacute to chronic cerebral infarction patients and 11 controls. All six infarcts containing lactate were alkalotic ($\text{pH}_i = 7.20 \pm 0.04$ vs. 7.05 ± 0.01 contralateral, $p < 0.01$). This finding of elevated lactate and alkalosis in chronic infarctions does not support the presence of chronic ischemia; however, it is consistent with the presence of phagocytic cells, gliosis, altered buffering mech-

anisms, and/or luxury perfusion. Total ^1H and ^{31}P metabolites were markedly reduced (about 50% on average) in subacute and chronic brain infarctions ($p < 0.01$), and N-acetyl aspartate (NAA) was reduced more (~75%) than other metabolites ($p < 0.01$). Because NAA is localized in neurons, selective NAA reduction is consistent with pathological findings of a greater loss of neurons than glial cells in chronic infarctions. **Key Words:** Brain infarction—Lactate—Alkalosis—Magnetic resonance spectroscopic imaging—Phosphorus metabolism—Hydrogen metabolism.

Brain cell metabolism depends on the blood supply of glucose and oxygen substrates. When blood supply to the brain becomes inadequate, anaerobic glycolysis of limited glucose stores produces lactic acidosis, which damages vascular endothelium, glia, and especially neurons (Plum, 1983; Kelly, 1985).

Previous ^1H magnetic resonance spectroscopy (MRS) studies have detected decreased N-acetyl

aspartate (NAA) and elevated lactate in chronic human brain infarcts (Berkelbach et al., 1988; Bruhn et al., 1989; Howseman et al., 1990; Duijn et al., 1992). NAA appears to be a specific neuron marker (Nadler and Cooper, 1972; Birken and Oldendorf, 1989; Gill et al., 1989). Persistent ischemia would be expected to produce elevated lactate and decreased pH_i (i.e., lactic acidosis), as observed in acute infarcts (Chang et al., 1990). However, alkalosis was detected in some chronic infarcts by ^{31}P MRS studies (Levine et al., 1988; Nakada et al., 1991; Sapey-Mariniere et al., 1992; Hugg et al., 1992). Therefore, the goal of this study was to investigate lactate and pH_i distributions in subacutely and chronically infarcted human brains.

Magnetic resonance spectroscopic imaging (MRSI) using phase encoding (Kumar et al., 1975; Brown et al., 1982; Maudsley et al., 1983) has an important advantage over MRS volume-selection localization techniques: MRSI simultaneously obtains spectra from multiple regions. Recently, sev-

Received March 22, 1992; final revision received March 23, 1992; accepted 25, 1992.

Address correspondence and reprint requests to Dr. Gerald B. Matson, at MR Unit, DVA Medical Center, 4150 Clement Street (11M), San Francisco CA 94121, U.S.A.

Abbreviations used: Cho, choline; Cr, creatine; FOV, field of view; HMPT, hexamethylphosphorotriamide; Lac, lactate; MCA, middle cerebral artery; MDPA, methylene diphosphonic acid; MRI, magnetic resonance imaging; MRSI, MR spectroscopic imaging; NAA, N-acetyl aspartate; OAM, orbital-auditory meatus; P_i, inorganic phosphate; PCr, phosphocreatine; PDE, phosphodiester; PME, phosphomonoester; PET, positron emission tomography; RF, radio frequency; VOI, volume of interest; WEFT, water-eliminated Fourier transform.

eral investigators have demonstrated the clinical feasibility of ^1H and ^{31}P MRSI (Twieg et al., 1989; Segebarth et al., 1990; Menon et al., 1990; Maudsley et al., 1990; Vigneron et al., 1990; Hugg et al., 1992; Duijn et al., 1992). In the present studies MRSI was used to map spatial distributions of ^1H and ^{31}P metabolites in cerebral infarction patients. Spatial correlations of lactate and pH_i were used to investigate the possibility that elevated lactate and alkalosis are spatially coincident in chronic infarctions.

METHODS

Human subjects

Twenty-two subjects were studied: 11 patients with nonhemorrhagic subacute to chronic (5 days to 2 years) cerebral infarction (five men, six women, ages 54 to 83 yr) and 11 normal controls (five men, six women, ages 26 to 54 yr). Eight of the 11 patients overlap another report (Duijn et al., 1992) limited to ^1H MRSI results. None of the controls overlap. Patients were referred from Letterman Army Hospital and the Department of Veterans Affairs Medical Center, San Francisco. Study protocols were approved by the University of California at San Francisco Human Research Committee, and written informed consent was obtained prior to each study.

MRI protocol

The magnetic resonance imaging (MRI) and MRSI studies were conducted with a Gyroscan S15 whole-body imaging and spectroscopy system (Philips Medical Systems, Shelton CT) operated at 2 T. Proton MR images of the head were first obtained: 7 sagittal locator slices (7 mm thick, 1.4 mm gap, $T_R = 450$ ms, $T_E = 30$ ms) and 18 oblique transaxial slices (5 mm thick, 1 mm gap, $T_R = 2000$ ms, $T_E = 30$ and 90 ms). These transaxial slices were obliquely angulated 20° supraorbitally beyond the orbital-auditory meatal (OAM) plane observed on the sagittal locator slices, giving a consistent anatomical perspective and facilitating comparisons between patients and controls. The angulation also diminished contamination of ^1H spectra by lipid in the orbital muscles.

^1H MRSI study protocol

For the ^1H MRSI studies, standard Philips spectroscopy acquisition software and a saddle-type imaging headcoil were employed (Duijn et al., 1992). Using the MR images to prepare for the ^1H MRSI study, a 2-cm-thick angulated slab volume of interest (VOI) was selected to encompass as much as possible of the infarct region and to avoid lipid in the skull and scalp. Typical VOI dimensions were 10×10 (transaxial plane) $\times 2$ cm. The optimal radiofrequency (RF) pulse amplitude for ^1H MRSI was determined by minimizing the water signal immediately following the second refocusing pulse in the double spin-echo sequence. The B_0 magnetic field was then shimmed (nonlocalized) using the ^1H imaging saddle coil to a water resonance linewidth of less than 15 Hz (0.17 ppm at 86 MHz).

The double spin-echo (PRESS) sequence (Ordidge et al., 1985; Bottomley, 1987) was used for VOI localization

in combination with water suppression and 2D gradient phase-encoding MRSI (Segebarth et al., 1990). The VOI localization sequence employed amplitude-modulated RF pulses in combination with slice selection gradients. Gradient spoiler pulses flanking the two 180° refocusing pulses were applied to reduce spurious transverse magnetization created by these pulses. The echo was sampled with a 1-kHz bandwidth beginning shortly after the last gradient pulse with 21% (108 ms) of the 512-ms sampling interval occurring before the echo center at $T_E = 272$ ms. The double spin-echo sequence was executed without water suppression for adjustment of the gradient spoiler pulses ("gradient tuning") to maximize the water echo signal. Localized B_0 shimming was next performed, typically resulting in a water resonance linewidth of 6 Hz (0.07 ppm) or less.

Two water-eliminated Fourier transform (WEFT) water suppression pulses (Patt and Sykes, 1972) preceded the start of the VOI localization sequence with delay times t_1 and t_2 which empirically minimized longitudinal water magnetization. The pulses were frequency-selective adiabatic inversion pulses with 50-Hz bandwidth centered on the water resonance. Gradient spoiler pulses dispersed spurious transverse magnetization excited by imperfect longitudinal inversion. The double WEFT sequence was found to be more effective for suppressing the water resonance than a single WEFT sequence, presumably because the tissue water T_1 relation was not a single exponential. Typically, $t_1 = 800$ ms (ranging from 750 to 830 ms in various subjects) and $t_2 = 50$ ms were used with a repetition time $T_R = 2$ s.

Finally, a 2D ^1H MRSI study was performed using 16×16 gradient phase-encoding steps over a field of view (FOV) just encompassing the skull, typically $(18 \text{ cm})^2$. The phase-encoding gradients were applied between the 90° excitation pulse and the first 180° refocusing pulse of the double spin-echo sequence. Four acquisitions were averaged for each phase-encoding step with phase-cycled excitation pulses. Total acquisition time was 34 min.

^{31}P MRSI study protocol

Following the ^1H MRSI study, the subject was removed from the magnet bore and allowed to rest about 10 min while the ^{31}P MRSI study was prepared. For accurate repositioning of the subject's head, a vacuum-assisted head holder, padded straps, and fiducial markings (forehead and temple on paper tape) using the Gyroscan laser alignment system were employed. A 3-ml external registration sample of methylene diphosphonic acid (MDPA, Sigma Chemical Co., St. Louis MO) was usually affixed to the subject's forehead or temple. This sample appeared on one slice in both ^1H MR images and ^{31}P MRS images.

Custom acquisition software was written to perform the ^{31}P MRSI studies (Hugg et al., 1992). An inductively coupled high-pass birdcage head coil with a Faraday shield and RF mirror was constructed and operated in a quadrature B_1 polarization mode (Hugg et al., 1990). The coil provided homogeneous RF excitation and detection with good sensitivity and homogeneity. The RF pulse length for ^{31}P MRSI was determined by observing the signal from a 3 ml sample of hexamethylphosphorotriamide (HMPT, Sigma) placed at the vertex of the head on the birdcage coil axis. The 3D ^{31}P MRSI study was performed with $12 \times 12 \times 12$ gradient phase-encoding steps and a short T_E spin-echo acquisition (Maudsley et al., 1990). The same angulation was used as in the pre-

ceding MRI and ^1H MRSI studies. The bipolar phase-encoding gradient pulses (1 ms duration, triangular, maximum strength 1.2 mT/m) were positioned symmetrically about the 180° RF refocusing pulse. The signal was sampled beginning with the echo center ($T_E = 3.5$ ms).

To optimize signal collection efficiency, partial-tip angle RF excitation and rapid pulse sequence repetition were used (Becker et al., 1979). An average $T_1 = 1.9$ s was assumed for tissue phosphocreatine (PCr) and inorganic phosphate (P_i) (Hubesch et al., 1990). For $T_R = 350$ ms, the optimal partial-tip angle for FID acquisition would be $\alpha = 34^\circ$ (Ernst et al., 1987). The pulse sequence employed an excitation pulse angle of $180^\circ - \alpha = 146^\circ$ with a single 180° -refocusing pulse, resulting in an effective partial-tip angle of $\alpha = 34^\circ$ (Hugg et al., 1992).

The 180° -pulse lengths were short enough (typically ≤ 250 μs) that off-resonance attenuation of signal was measured to be less than 10% at the phosphomonoester (PME) and β -ATP resonances. The carrier frequency was set at -5.0 ppm ($\delta\text{PCr} = 0$ ppm reference), about midway between γ -ATP and α -ATP, and thus about midway between the outer spectral limits of interest at PME (6.4 ppm) and β -ATP (-16.4 ppm). Four acquisitions were averaged for each phase-encoding step with phase-cycled refocusing pulses. Total acquisition time was 40 min.

MRSI processing and display

MRS images were reconstructed (Maudsley et al., 1992) using Fourier transforms with apodization and zero filling to 32×32 interpolated voxels in one (^1H , 2 cm thick) or 16 (^{31}P , 1.7 cm thick) interpolated transaxial planes. The nominal in-plane resolution before spatial filtering was 1.125 cm (^1H) or 2.25 cm (^{31}P) and the nominal voxel size was 2.5 cm 3 (^1H) or 11 cm 3 (^{31}P). Mild gaussian spatial smoothing produced an effective in-plane resolution of about 1.4 cm (^1H) or 2.9 cm (^{31}P) and an effective voxel size of about 3.9 cm 3 (^1H) or 25 cm 3 (^{31}P). The MRS images were linearly interpolated to 64×64 voxels for display. Spectral line broadening of 1 Hz (^1H) or 15 Hz (^{31}P) was used. For ^{31}P spectra a 150-Hz convolution difference filter was used to remove broad spectral signal from less mobile metabolites.

Total metabolite images were generated by total spectral integration during reconstruction. Additional images of individual metabolites were produced during interactive display and analysis by spectral integration over individual resonances. Because some of the ^{31}P spectral lines partially overlapped, completely separated metabolite maps of the overlapping resonances were not derived. Metabolite maps were scaled individually for display. The display software (Maudsley et al., 1992) provided for simultaneous display and spatial registration of the MR and metabolite images. Regions for spectral examination were selected by mouse control of a cursor on either MR or metabolite images.

To register the anatomical location of metabolite dis-

tributions in MRS images, these images were often overlaid by a high-pass filtered T_2 -weighted proton MR image, which delineated high-contrast tissue edges, such as ventricles, sulci, skull, and infarction region (Fig. 1b, c, and d).

Spectral fitting

Individual ^1H or ^{31}P spectra selected from the full MRSI study data sets were fit by a least squares method (NMR1 program, New Methods Research, Syracuse NY). Spectra were interpolated by zero-filling and Fourier transformation to a digital resolution of 0.5 Hz/point (^1H) or 3 Hz/point (^{31}P). For ^1H spectra, choline (Cho), creatine + phosphocreatine (Cr), *N*-acetyl aspartate (NAA), and lactate (Lac) peaks were identified by their chemical shifts (Frahm et al., 1989). For ^{31}P spectra, phosphomonoesters (PME), inorganic phosphate (P_i), phosphodiester (PDE), phosphocreatine (PCr), and three phosphorus resonances of adenosine triphosphate (γ -, α -, and β -ATP) were identified (Hubesch et al., 1990). Proton magnitude spectra were fit, with lactate being fit by a doublet with 7-Hz splitting. Initially, spectra were fit with lorentzian, then gaussian lineshapes for comparison. The gaussian lineshapes fit better and were therefore used to determine chemical shifts and metabolite peak integrals. Intracellular pH_i was derived from the curve-fitted chemical shift δP_i referenced to $\delta\text{PCr} = 0$ ppm (Petroff et al., 1985a).

Peak integrals of spectra from infarct and contralateral reference regions were used to determine metabolite ratios. The infarct region was identified from the higher spatial resolution proton MR images. The reference spectra were extracted from the homologous region of the contralateral hemisphere. In recognition of the spatial point-spread function, VOI chemical-shift artifact (^1H MRSI), and to minimize contamination by other tissues (partial-volume effects), spectra were extracted from regions well inside the selected tissue type and away from the edges of the ^1H VOI. Although eight patients were common to this combined ^1H and ^{31}P MRSI study and another report limited to ^1H MRSI results (Duijn et al., 1992), the selection and fitting of ^1H spectra were independent in the two studies. The spectra in this study were not quantitated to estimate metabolite concentrations. A quantitation method for ^{31}P MRSI has subsequently been developed (Matson et al., 1991), and a quantitation method for ^1H MRSI is under development. Statistical comparison of infarcted, contralateral, and control regions was performed with *t*-tests corrected for multiple comparisons, where $p < 0.05$ was considered significant.

RESULTS

Total ^1H and ^{31}P metabolite images of all controls were relatively uniform throughout the brain parenchyma with bilateral symmetry. Marked deviations

FIG. 1. MRSI study of a 76-year-old woman with a 2-year-old right MCA territory infarction. (a) T_2 -weighted transaxial MR image. The blue box within the brain parenchyma outlines the $10 \times 9 \times 2$ cm 3 thick VOI selected for ^1H MRSI. (b) NAA metabolite map with high-pass filtered MR image superposed in red. The color scale is shown beside the MRS image. Two single effective voxels (open squares, 4 cc each) were selected for spectral analysis in the right parietal infarct and in the left homologous contralateral region. (c) Lactate metabolite map. The color scale was adjusted to highlight the relatively weak lactate signals in the presence of the intense lipid signal contamination along the skull. Lactate was observed in the infarct and in the periventricular region. (d) Total ^{31}P metabolite map. Two single effective voxels (open squares, 25 cc each) were selected for spectral analysis. (e) The two selected ^1H spectra: right infarcted region (bottom) compared with the left contralateral region (top). (f) The two selected ^{31}P spectra: right infarcted region (bottom) compared with the left contralateral region (top).

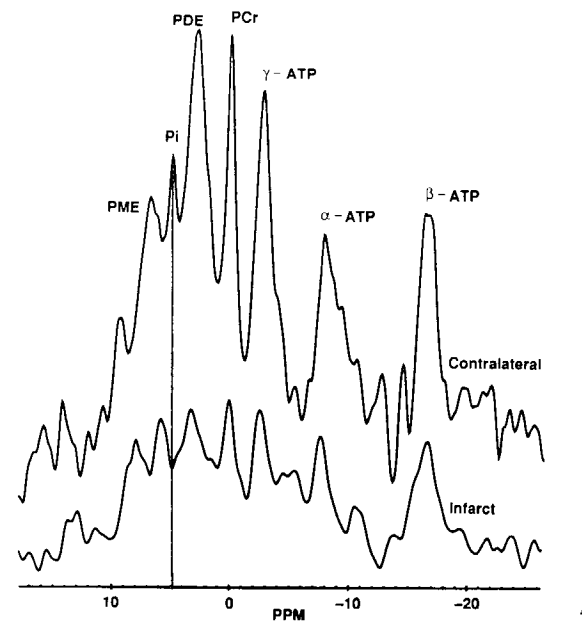
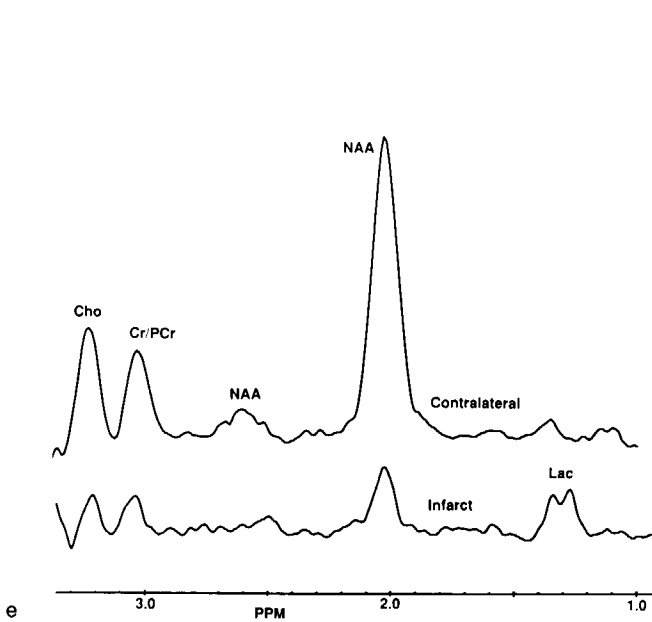
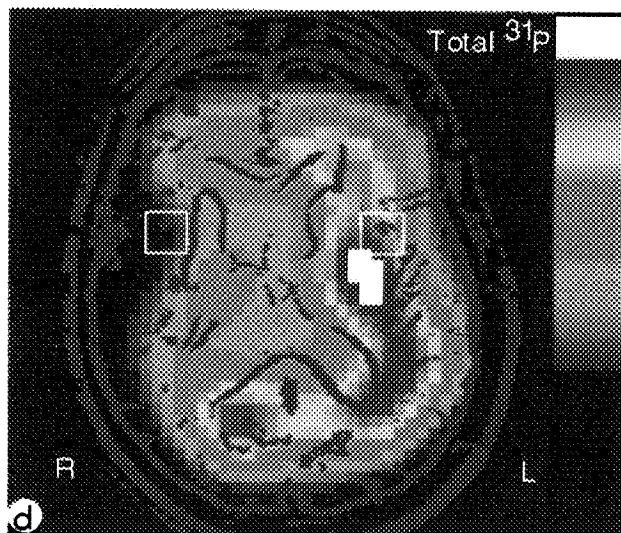
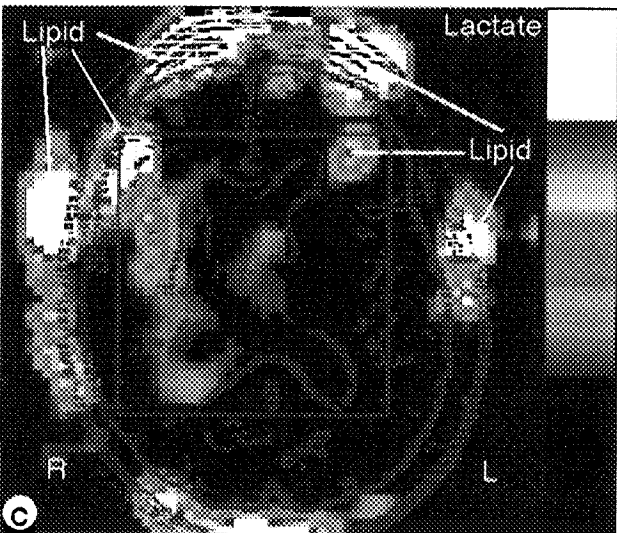
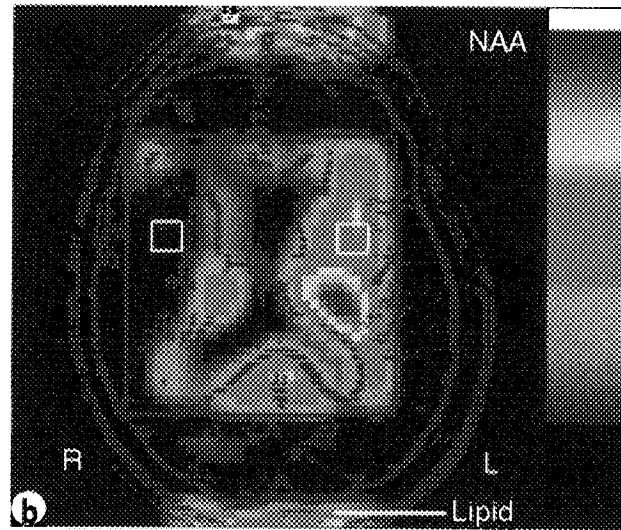
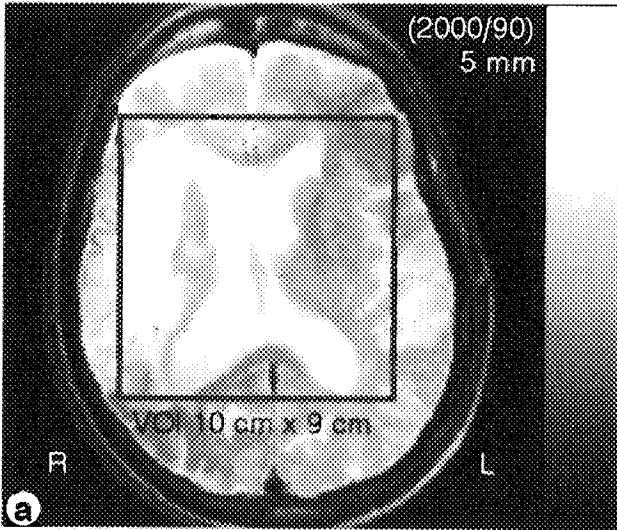


TABLE 1. Cerebral infarct patients studied by ^1H & ^{31}P MRSI ($n = 11$)

Age/sex	Infarct age (days)	Infarct size ^a	Infarct location ^b	Lactate ^c
63 M	5	S	L internal capsule, putamen	I
73 M	6 & 300	S	Multiple periventricular WM	PV
66 F	7	M	L occipital-parietal deep WM	PV
83 M	10 & 600	M	R PCA-MCA border zone	PV
70 M	300	M	R centrum semiovale	PV
72 M	400	M	R PCA-MCA border zone	PV
79 F	10	L	R MCA territory	I, PV
54 M	200	L	R MCA territory	I, PV
75 F	400	L	R MCA territory	I, PV
76 F	600	L	R MCA territory	I, PV
76 F	700	L	L MCA territory	I, PV

^a Maximum diameter: S = small (<2 cm), M = medium (2 to 4 cm), L = large (>4 cm).

^b PCA = posterior cerebral artery, MCA = middle cerebral artery, WM = white matter.

^c Lactate in: I = infarct, PV = periventricular region.

from uniform bilateral symmetry were seen only in the infarction patients. Metabolite patterns (mol %, described below) for controls are listed in Table 2.

Table 1 lists the patients by age, sex, infarct age, size, and location of infarct region as measured on T_2 -weighted MR images. The patient list is divided into two groups: six small to medium-sized primarily deep white matter infarcts and five large middle cerebral artery (MCA) territory infarcts with cortical involvement. Also indicated is the presence of elevated lactate detected by ^1H MRSI within the infarction and/or the periventricular region. All five large MCA infarcts contained elevated lactate in both the infarcted and periventricular regions. One small subacute (5 days) infarct in the internal capsule/putamen region also contained elevated lactate. All other small to medium white matter infarcts contained elevated lactate in the periventricular region only.

The MRSI study of a 76-year-old woman with a 2-year-old right MCA territory infarction is illustrated in Fig. 1. The T_2 -weighted MR image shown in Fig. 1a is characterized by the hyperintense infarction region in the right parietal lobe and an enlarged right ventricle. The blue box within the brain parenchyma outlines the $10 \times 9 \times 2 \text{ cm}^3$ VOI selected for ^1H MRSI. The NAA metabolite map is shown in Fig. 1b with a high-pass filtered MR image superposed in red. Hypointense signal corresponds to CSF in the ventricles and to the infarcted region. Some lipid contamination is localized along the skull. Two single effective voxels (4 cc each) were selected for spectral analysis in the right parietal infarct and in the left homologous contralateral region. The lactate (+ lipid) metabolite map is shown in Fig. 1c. The color scale was adjusted to highlight the relatively weak lactate signals in the presence of the intense lipid signal contamination around the skull. Lactate was observed in the infarct and in the

periventricular region. The total ^{31}P metabolite map is shown in Fig. 1d. Two single effective voxels (25 cc each) were selected for spectral analysis. The two selected ^1H spectra are shown in Fig. 1e, where the infarcted region spectrum shows greatly diminished choline, creatine, and NAA, as well as increased lactate compared to the contralateral region spectrum. The two selected ^{31}P spectra are shown in Fig. 1f, where the infarcted region spectrum shows greatly diminished phosphorus metabolites, as well as an alkaline (leftward) shift of the P_i peak compared to the contralateral region spectrum.

The normalized ^{31}P and ^1H MRSI metabolite ratios for all patients are listed in the second column of Table 2. The ratio of the infarct peak integral divided by the contralateral peak integral is given for each metabolite. All metabolite signals (except P_i) were significantly reduced ($p < 0.01$) in the infarcts compared to contralateral reference regions. The reduction of NAA in the infarcts was significantly greater than the reductions of total phosphorus, choline, or creatine ($p < 0.01$). The last three columns list the metabolite patterns (i.e., the distribution of ^{31}P or ^1H among the various metabolites = each metabolite/ $^{31}\text{P}_{\text{tot}}$ or $^1\text{H}_{\text{tot}}$, sometimes called "mol %") in the infarcted regions, contralateral regions, and matched regions of the controls. There was no significant difference in phosphorus metabolite patterns between infarcted, contralateral, and control regions. There was a significant difference ($p < 0.01$) in ^1H metabolite patterns between infarcted and contralateral regions. Infarcts had more choline and less NAA as a fraction of total proton metabolites. There was no significant ^1H metabolite pattern difference between the patient contralateral regions and the controls.

The intracellular pH (pH_i) measured by ^{31}P MRSI in infarcts is shown as a function of infarct age in Fig. 2, including nine previously published mea-

TABLE 2. ^{31}P and ^1H MRSI metabolite ratios and patterns in cerebral infarctions and controls^a

Metabolite	Infarct/contralateral	Metabolite/Total (infarct) ^b	Metabolite/Total (contralateral) ^b	Metabolite/Total (controls) ^b
P _i	95 ± 62	7 ± 4	6 ± 3	10 ± 3
PCr	46 ± 11*	21 ± 6	21 ± 2	20 ± 2
ATP	62 ± 25*	22 ± 7	17 ± 2	13 ± 2
PME	56 ± 44*	18 ± 7	19 ± 7	17 ± 6
PDE	42 ± 21*	32 ± 7	37 ± 7	40 ± 7
Choline	56 ± 40*†	39 ± 9§	25 ± 5	25 ± 5
Creatine	42 ± 33*†	21 ± 3	18 ± 3	17 ± 3
NAA	26 ± 24*	40 ± 10§	57 ± 7	58 ± 6

Paired *t*-tests ($p < 0.01$): *Infarct signal < contralateral signal, †Choline, creatinine signal decrease < NAA signal decrease, §Infarct pattern ≠ contralateral pattern.

^a Values (%) ± SD ($n = 11$ patients, 11 controls).

^b Metabolite patterns ("mol %"): Metabolite/ $^{31}\text{P}_{\text{total}}$ corrected for saturation (Hugg et al., 1992); metabolite/ $^1\text{H}_{\text{total}}$ not corrected for saturation.

surements (^{31}P only, no overlap with current study subjects; Hugg et al., 1992). The six infarcts in this study which contained lactate are represented by filled circles, and the five without lactate by open circles. Eleven controls had $\text{pH}_i = 7.01 \pm 0.02$, represented by a dashed line. Most subacute infarcts were acidotic, while most chronic infarcts were alkalotic.

The intracellular pH_i measured by ^{31}P MRSI in infarcted regions, contralateral regions, and controls is shown in Fig. 3. The first grouping of six patients (five large MCA territory infarcts and one small subacute infarct) had elevated lactate within the infarct. All six had higher pH_i ($p = 0.01$) within the infarcted regions (7.20 ± 0.04) than in the homologous contralateral regions (7.05 ± 0.02). The second grouping of five patients (small to medium deep white matter infarcts) had no elevated lactate in the infarct. No significant mean difference was found in the second group infarcted regions ($\text{pH}_i = 6.98 \pm 0.04$) compared to the homologous contralateral regions (7.03 ± 0.04). Control $\text{pH}_i = 7.01 \pm 0.02$ ($n = 11$) is represented by a dashed line and datum.

DISCUSSION

The major finding of this study was that all six subacute or chronic infarcts containing lactate were alkalotic. Other findings confirmed previous reports (Sappey-Marini et al., 1992; Duijn et al., 1992): ^1H and ^{31}P metabolites were markedly reduced in subacute and chronic brain infarctions, and NAA was reduced more than other metabolites.

Elevated lactate and alkalosis

Six patients had elevated lactate within the infarct and 10 patients had elevated lactate in the periventricular region. This finding substantiates

previous reports which suggested that lactate concentrations may be elevated within or adjacent to subacute-to-chronic infarcts (Ott et al., 1990; Graham et al., 1991; Duijn et al., 1992). There are several possible explanations for the chronically elevated lactate.

One possibility is that the lactate is a stagnant pool produced during the acute phase of infarction. However, this is unlikely because lactate was present as long as two years postinfarction, and positron emission tomography (PET) studies have shown perfusion exceeding metabolic needs (i.e., luxury perfusion; Syrota et al., 1985; Senda et al., 1989) in chronic infarction regions. Furthermore, one ^1H MRS study of a 32-day-old infarction using labelled ^{13}C -glucose demonstrated continuing glycolytic lactate synthesis rather than simple loculation of a stagnant pool (Rothman et al., 1991).

A second possibility is that increased lactate results from continuing ischemia in the border zone of the infarction (i.e., an ischemic penumbra; Hakim, 1987). However, none of the eleven patients had increased lactate exclusively in the border zone of the infarct; no lactate "halo" was observed. Lactate was found throughout the infarcted region and/or within the periventricular region. If lactate is produced by viable, yet persistently ischemic tissue, then ischemia, which stimulates the anaerobic production of lactic acid from glucose, would be expected to produce lactic acidosis. The finding that all six subacute to chronic infarcts containing elevated lactate were alkalotic (Fig. 3) is inconsistent with the hypothesis of persistent ischemia. This finding of elevated lactate and alkalosis supports the PET finding that ischemia does not persist in subacute-to-chronic infarctions (Hakim, 1987).

A third possibility is that tissue alkalosis enhances glycolysis and lactate production (Ui, 1966).

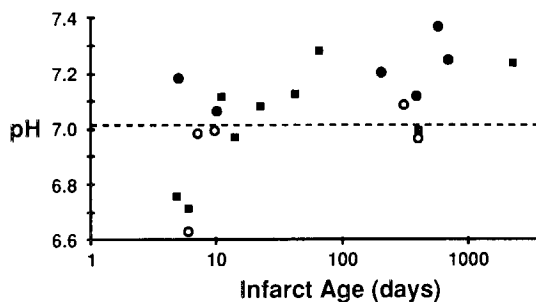


FIG. 2. Intracellular pH_i measured by ^{31}P MRSI in infarcts as a function of infarct age, including nine previously published measurements (filled squares; Hugg et al., 1992). Six infarcts containing lactate are represented by filled circles, five without lactate by open circles. Control $\text{pH}_i = 7.01 \pm 0.02$ is represented by a dashed line.

Anaerobic metabolism of glucose to pyruvate generates NADH, which shifts the cytosolic redox state, causing increased lactate production from pyruvate by lactate dehydrogenase. The major regulator of glycolysis is phosphofructokinase, which has an alkaline pH_i optimum (Kemp and Foe, 1983; Uyeda, 1979). Thus lactate production is stimulated by alkalosis. Brain lactate is elevated by the alkalosis produced during hypocapnia in animals (Kjallquist et al., 1969; Petroff et al., 1985b) and humans (van Ryen et al., 1989). Furthermore, hyperventilation of both animals (Raichle et al., 1970) and humans (van Nimmen et al., 1986) leads to respiratory alkalosis and increases brain glucose consumption and lactate production while O_2 consumption does not change. Thus, it is possible that persistent lactate is a secondary consequence of persistent alkalosis.

The finding of acidosis in subacute (5–7 days) infarctions and alkalosis in chronic (10+ days) infarctions (Fig. 2) is consistent with previous reports of pH_i “flip-flop” and “rebound” alkalosis in ischemic brain injury (Syrota et al., 1985; Hakim, 1986; Levine et al., 1988; Senda et al., 1989; Chopp et al., 1990a,b; Nakada et al., 1991). The cross-over from acute acidosis to chronic alkalosis has been observed most frequently in humans between the 3rd and 9th days postinfarction by serial ^{31}P MRS studies. Persistent alkalosis has been observed in chronic human brain infarction using a single-volume ^{31}P MRS technique (Sappey-Marini et al., 1992).

There are several possible explanations for chronic alkalosis. One possibility is that alkalosis is associated with CSF contributions. The infarcted region atrophies, resulting in ecephalomalacia or CSF-filled cyst formation with compensatory dilatation of nearby CSF spaces (Hachinski and Norris, 1985). The extracellular pH (pH_e) of CSF is higher than normal brain by 0.3 to 0.4 pH unit, but the CSF

concentration of phosphate is normally low (0.2 mM) (Siegel et al., 1989) and P_i is not detected in vivo in CSF above noise levels by ^{31}P MRS. If a significant portion of the P_i detected in the infarct regions is a remnant from the ischemic insult and subsequent necrosis of the affected cells, then one component of the measured pH might be associated with the extracellular CSF-filled infarct cyst rather than representing purely intracellular pH_i . The concentration of extracellular P_i is unknown in chronic infarcts. However, no significant splitting of the P_i resonance was observed in this study, so it is unlikely that a large amount of extracellular P_i (with pH_e different from pH_i) is present in chronic infarcts.

A second possibility is that alkalosis may be associated with the presence of phagocytes. Necrotic brain tissue containing inflammatory cells has been associated with alkalosis (Chopp et al., 1990b). Phagocytic cells (Kelly, 1985; Newsholme and Newsholme, 1989) have a high rate of anaerobic glycolysis (Karnovsky, 1962) leading to elevated lactate. Brain macrophages (microglia, astrocytes, and leucocytes) appear about 1 to 3 days after infarction and slowly disappear over many months (Garcia and Kamijyo, 1974). This lactate source is consistent with a case report of decreased NAA and increased lactate in 10- and 15-day-old infarcts, followed by patient death and autopsy 7 days later (Petroff et al., 1991). Histopathology showed predominantly foamy macrophages with few other cells throughout the infarction core regions, blending into border zones of reactive astrocytes with a scattering of ischemically necrotic neurons. Therefore, it is possible that phagocytes are responsible for alkalosis.

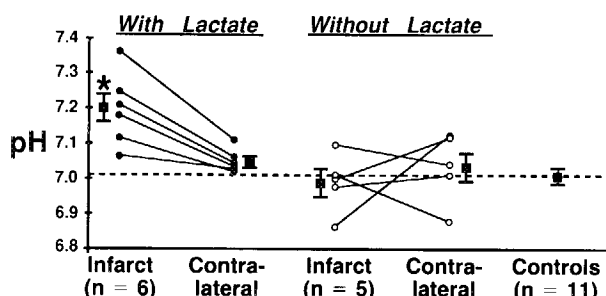


FIG. 3. Intracellular pH_i measured by ^{31}P MRSI in infarcted regions, contralateral regions, and controls. The first grouping shows six patients with lactate detected within the infarct. All six had higher pH_i ($p = 0.01$) within the infarcted regions ($\text{pH}_i = 7.20 \pm 0.05$) than in the homologous contralateral regions ($\text{pH}_i = 7.05 \pm 0.02$). The second grouping shows five patients without lactate in the infarct. No significant difference was found in the infarcted regions ($\text{pH}_i = 6.98 \pm 0.04$) compared to the homologous contralateral regions ($\text{pH}_i = 7.03 \pm 0.04$). Control $\text{pH}_i = 7.01 \pm 0.02$ is represented by a dashed line and datum.

A third possible cause of alkalosis is that glial cells proliferate to replace lost neurons in chronically infarcted regions (Hachinski and Norris, 1985). Astrocytes in normal brain have not been characterized by significantly elevated pH_i . However, alkalosis may be associated with the stimulation of glial cell growth. Growth factor increases pH_i in fibroblasts (Schuldiner and Rozengurt, 1982). Increased intracellular brain pH_i has been reported in glial tumors (Hubesch et al., 1990) and in mesial sclerosis which characterizes epileptogenic foci (Laxer et al., 1992).

A fourth possible mechanism for postinfarction cerebral alkalosis is altered pH_i maintenance mechanisms in the remaining viable cells. All vertebrate cells, including neurons and glia, contain a Na^+/H^+ antiporter system (Kulwich, 1983; Aronson, 1985). Ischemia and associated acute lactic acidosis could cause an adaptive increase in brain buffering by the Na^+/H^+ antiporter in remaining viable cells, similar to that observed in other tissue (Cohen et al., 1983; Adler et al., 1990; Raley-Susman et al., 1991), causing chronic infarctions to be more alkaline. In some cells Na^+ influx and growth factor stimulate the Na^+/H^+ antiporter to increase pH_i (Lagarde and Pouyssegur, 1986; Sardet et al., 1990). Thus, it is possible that altered buffering mechanisms may also contribute to alkalosis.

A fifth possible mechanism for postinfarction alkalosis has been suggested by PET studies (Syrota et al., 1985; Hakim et al., 1987; Senda et al., 1989) in which a significant pH_i increase in subacute-to-chronic infarcts correlated with a reduced oxygen extraction fraction and blood perfusion exceeding metabolic demand (i.e., luxury perfusion), causing alkalosis by removing excess CO_2 (Fox et al., 1988). Although luxury perfusion and resultant alkalosis have been demonstrated in subacute and early chronic infarctions, it is not known how long luxury perfusion persists. If local luxury perfusion persists in chronic infarctions, then it possibly may contribute to alkalosis and the stimulation of glycolytic lactate synthesis.

Metabolite loss

The deficit of proton and phosphorus metabolite signals (Table 2) is consistent with pathological findings that brain infarction is associated with gliosis and a marked decrease of cellular density (Garcia and Kamijyo, 1974; Hachinski and Norris, 1985). The reduction of metabolite signals is also consistent with previous studies using ^1H and ^{31}P MRS techniques (Welch et al., 1985; Bottomley et al., 1986; Brant-Zawadzki et al., 1987; Levine et al., 1988; Berkelbach et al., 1988; Hubesch et al., 1989;

Weiner et al., 1989; Houkin et al., 1989; Bruhn et al., 1989; Sappey-Mariniere et al., 1992; Hugg et al., 1992; Duijn et al., 1992).

Selective NAA loss

Evidence suggests that NAA is specifically localized in neuronal cytosol (Nadler and Cooper, 1972; Birken and Oldendorf, 1989; Petroff et al., 1989), whereas choline and creatine are found in both neurons and glia (Gill et al., 1989). The finding (Table 2) that NAA was reduced more (about 75% average) than all other metabolites (about 50% on average) is consistent with pathological findings of a greater loss of neurons than glial cells within infarctions (Garcia and Kamijyo, 1974; Hachinski and Norris, 1985). The lack of significant difference between mean phosphorus metabolite patterns (mol %) in infarcted, contralateral, and control regions suggests that the phosphorus metabolite patterns for neurons, glia, and macrophages are quite similar, because the cell population has substantially changed. The significantly greater choline fraction in infarcts may reflect the presence of macrophages in the infarcted region, because they contain choline but little, if any, NAA or creatine (Petroff et al., 1991). Another possibility is that increased choline may reflect altered phospholipid metabolism, because mobile choline (NMR observable) can be released through catabolism of phospholipid membranes.

Limitations of MRSI

Low S/N and limited spatial resolution. The low sensitivity of ^{31}P MRS and the low concentrations of ^{31}P metabolites limit the spatial resolution of ^{31}P MRSI. Even at the relatively low spatial resolution (2.9 cm in-plane) used in these studies, single effective voxel (25 cc) S/N was low (8 to 12 for PCr). The point-spread function is inherently broad with ringing tails because of the low number of phase encodings. Therefore, mild spatial filtering was applied during MRSI reconstruction to reduce ringing and intervoxel contamination significantly, while only moderately degrading the spatial resolution. Lactate detected in the periventricular region, for example, could have been located in periventricular brain tissue and/or in the CSF of the ventricles. For the medium (2 to 4 cm maximum diameter) to large (>4 cm) infarctions, there was close correspondence in total metabolite reduction measured by ^{31}P MRSI and the higher spatial-resolution ^1H MRSI. Thus, when the infarction was larger than the spatial resolution, a relatively uncontaminated measurement could be made by selecting an effective voxel wholly within the infarcted region. Only for the two small (<2 cm) infarctions did the ^{31}P MRSI

measurement significantly underestimate total phosphorus metabolite reduction because of partial volume contribution from surrounding viable tissue.

Water/lipid contamination. A major difficulty with in vivo ^1H MRS studies is the presence of intense resonances of water and lipid which interfere with the metabolite resonances of interest. Although our acquisition method suppressed most of these unwanted signals, often some water and lipid signal contamination remained, especially in spectra from regions close to the skull. In a "lactate + lipid" image (Fig. 1c), spectra within the VOI usually showed the characteristic lactate doublet with 7 Hz splitting at 1.3 ppm (Fig. 1e), but spectra around the skull outside the VOI showed a much broader signal characteristic of lipid (from about 1.0 to 2.5 ppm).

Eddy currents. During switching of B_0 magnetic field gradients, eddy currents are induced in the conductive parts of the magnet, creating serious effects for ^1H MRSI (Duijn et al., 1992). Because eddy currents produce spatially variable phase distortion, ^1H magnitude spectra were used. Gradient tuning (see Methods) was used to minimize dynamic interference of eddy currents with shimming.

B_1 inhomogeneity. Total ^1H and ^{31}P metabolite images of all controls were relatively uniform throughout brain parenchyma with bilateral symmetry. Marked deviations from uniform bilateral symmetry were seen only in the infarction patients. The ^{31}P birdcage resonator B_1 field was quite homogeneous, but the ^1H saddle-type imaging coil had significant B_1 field inhomogeneities which degraded the water suppression, VOI slice profiles, and the sensitivity of signal reception. Improvements will be made by constructing a ^1H birdcage resonator.

Chemical shift artifact. The VOI positions (but not the MRSI voxel positions) were offset spatially for the various ^1H metabolites due to the well-known chemical shift artifact. Therefore, we selected no spectra near the VOI edges.

CONCLUSION

These findings suggest no evidence of chronic ischemia; however, elevated lactate and alkalosis in chronic infarctions is consistent with the presence of phagocytic cells, gliosis, altered buffering mechanisms, and/or luxury perfusion. ^1H and ^{31}P MRSI metabolite images provide information beyond that obtained by MRI, suggesting that MRSI has considerable potential clinical value, especially for therapy and prognosis of acute brain infarctions.

Acknowledgment: This work was supported by NIH grants HL07192 (JWH through the UCSF Cardiovascular

Research Institute), R01-DK33293 (MWW), and R01-CA48815 (AAM), Philips Medical Systems, the Department of Veterans Affairs Medical Research Service (MWW), and the American Association of Retired Persons Andrus Foundation (MWW). The cooperation and consultation of the following DVA Medical Center physicians who referred patients for this study is gratefully acknowledged: SL Graham, J Grotta, and M Greenberg. Valuable assistance was rendered by RS Lara, E Lin, M Elliott, and SK Steinman.

REFERENCES

- Adler S, Simplaceanu V, Ho C (1990) Brain pH in acute isocapnic metabolic acidosis and hypoxia: a ^{31}P NMR study. *Am J Physiol* 258:F34-F40
- Aronson PS (1985) Kinetic properties of the plasma membrane $\text{Na}^+ - \text{H}^+$ exchanger. *Annu Rev Physiol* 47:545-560
- Becker ED, Ferretti JA, Gambhir PB (1979) Selection of optimum parameters for pulse Fourier transform nuclear magnetic resonance. *Anal Chem* 51:1413-1420
- Berkelbach van der Sprenkel JW, Luyten PR, van Rijen PC, Tulleken CAF, den Hollander JA (1988) Cerebral lactate detected by regional proton magnetic resonance spectroscopy in a patient with cerebral infarction. *Stroke* 19:1556-1560
- Birken DL, Oldendorf WH (1989) N-acetyl-L-aspartic acid: a literature review of a compound prominent in ^1H -NMR spectroscopic studies of brain. *Neurosci Biobehav Rev* 13: 23-31
- Bottomley PA (1987) Spatial localization in NMR spectroscopy in vivo. *Ann NY Acad Sci* 508:333-348
- Bottomley PA, Drayer BP, Smith LS (1986) Chronic adult cerebral infarction studied by phosphorus NMR spectroscopy. *Radiology* 160:763-766
- Brant-Zawadzki M, Weinstein P, Bartowski H, Moseley M (1987) MR imaging and spectroscopy in clinical and experimental ischemia: a review. *Am J Neuroradiol* 8:39-48
- Brown TR, Kincaid BM, Ugurbil K (1982) NMR chemical shift imaging in three dimensions. *Proc Natl Acad Sci USA* 79: 3523-3526
- Bruhn H, Frahm J, Gyngell ML, Merboldt KD, Hänicke W, Sauter R (1989) Cerebral metabolism in man after acute stroke: new observations using localized proton NMR spectroscopy. *Magn Reson Med* 9:126-131
- Chang LH, Shirane R, Weinstein PR, James TL (1990) Cerebral metabolic dynamics during temporary complete ischemia in rats monitored by time-shared ^1H and ^{31}P NMR spectroscopy. *Magn Reson Med* 13:6-13
- Chopp M, Vande Linde AMQ, Chen H, Knight R, Helpert JA, Welch KMA (1990a) Chronic intracellular cerebral alkalosis after an 8 minute forebrain ischemic insult in the rat. *Stroke* 21:463-466
- Chopp M, Chen H, Vande Linde AMQ, Brown E, Welch KMA (1990b) Time course of postischemic intracellular alkalosis reflects the duration of ischemia. *J Cereb Blood Flow Metab* 10:860-865
- Cohen DE, Klahr S, Hammerman MR (1983) Metabolic acidosis and parathyroidectomy increase $\text{Na}^+ - \text{H}^+$ exchange in brush border vesicles. *Am J Physiol* 245:F217-F222
- Duijn JH, Matson GB, Maudsley AA, Hugg JW, Weiner MW (1992) Proton magnetic resonance spectroscopic imaging of human brain infarction. *Radiology* 183:711-718
- Ernst RR, Bodenhausen G, Wokaun A (1987) *Principles of Nuclear Magnetic Resonance in One and Two Dimensions*. New York, Oxford University Press, pp 124-125
- Fox PT, Raichle ME, Mintum MA, Dence C (1988) Nonoxidative glucose consumption during focal physiologic neural activity. *Science* 241:462-464
- Frahm J, Bruhn H, Gyngell ML, Merboldt KD, Hänicke W, Sauter R (1989) Localized proton NMR spectroscopy in dif-

- ferent regions of the human brain in vivo: relaxation times and concentrations of cerebral metabolites. *Magn Reson Med* 11:47-63
- Garcia JH, Kamijyo Y (1974) Cerebral infarction: evolution of histopathological changes after occlusion of a middle cerebral artery in primates. *J Neuropathol Exp Neurol* 33:408-421
- Gill SS, Small RK, Thomas DGT, Patel P, Porteous R, Van Bruggen N, Gadian DG, Kauppinen RA, Williams SR (1989) Brain metabolites as ^1H NMR markers of neuronal and glial disorders. *NMR Biomed* 2:196-200
- Graham GD, Howseman AM, Rothman DL, Lantos G, Fayad PB, Brass LM, Petroff OAC, Shulman RG, Prichard JW (1991) Proton magnetic resonance spectroscopy of metabolites after cerebral infarction in humans. *Stroke* 22:143
- Hachinski V, Norris JW (1985) *The Acute Stroke*. Philadelphia, FA Davis, pp 41-63, 227-243
- Hakim AK (1986) Cerebral acidosis in focal ischemia. II. Nimodipine and verapamil normalize cerebral pH following middle cerebral artery occlusion in rat. *J Cereb Blood Flow Metab* 6:676-683
- Hakim AK (1987) The cerebral ischemic penumbra. *Can J Neurol Sci* 14:557-559
- Hakim AM, Pokrupa RP, Villanueva J, Diksic M, Evans AC, Thompson CJ, Meyer E, Yamamoto YL, Feindel WH (1987) The effect of spontaneous reperfusion on metabolic function in early human cerebral infarcts. *Ann Neurol* 21:279-289
- Houkin K, Nakada T, Suzuki N, Kwee IL (1989) ^{31}P magnetic resonance spectroscopy of chronic cerebral infarction in rats. *NMR Biomed* 2:83-86
- Howseman AM, Graham GD, Rothman DL, Lantos G, Fayad PB, Brass LM, Petroff OAC, Shulman RG, Prichard JW (1990) A ^1H NMR study of cerebral lactate distribution following stroke. *Proc Soc Magn Reson Med* 9:1206
- Hubesch B, Sappey-Mariniere D, Hetherington HP, Twieg DB, Weiner MW (1989) ^{31}P MRS studies of human brain. *Invest Radiol* 24:1039-1042
- Hubesch B, Sappey-Mariniere D, Roth K, Meyerhoff DJ, Matson GB, Weiner MW (1990) P-31 MR spectroscopy of normal human brain and brain tumors. *Radiology* 174:401-409
- Hugg JW, Maudsley AA, Weiner MW, Matson GB (1990) Enhanced birdcage coil for ^{31}P spectroscopic imaging of human brains. *Proc Soc Magn Reson Med* 9:528
- Hugg JW, Matson GB, Twieg DB, Maudsley AA, Sappey-Mariniere D, Weiner MW (1992) ^{31}P Phosphorus MR spectroscopic imaging (MRSI) of normal and pathological human brains. *Magn Reson Imaging* 10:227-243
- Karonvsky ML (1962) Metabolic basis of phagocytic activity. *Physiol Rev* 42:143-168
- Kelly JP (1985) Reactions of neurons to injury. In: *Principals of Neural Science, 2nd Ed.* (Kandel ER, Schwartz J, eds), New York, Elsevier, pp 187-195
- Kemp RG, Foe LG (1983) Allosteric regulatory properties of muscle phosphofructokinase. *Mol Cell Biochem* 57:147-154
- Kjallquist A, Nardini M, Siesjö BK (1969) The regulation of extra- and intracellular acid-base parameters in the rat brain during hyper- and hypocapnia. *Acta Physiol Scand* 76:485-494
- Krulwich TA (1983) Na^+/H^+ antiporters. *Biochim Biophys Acta* 726:245-264
- Kumar A, Welti D, Ernst RR (1975) NMR Fourier zeugmatography. *J Magn Reson* 18:69-83
- Lagarde AE, Pouyssegur JM (1986) The $\text{Na}^+:\text{H}^+$ antiport in cancer. *Cancer Biochem Biophys* 9:1-14
- Laxer KD, Hubesch B, Sappey-Mariniere D, Weiner MW (1992) Increased pH and inorganic phosphate in temporal seizure foci demonstrated by ^{31}P MRS. *Epilepsia* 33:618-623
- Levine SR, Welch KMA, Helpert JA, Chopp M, Bruce R, Selwa J, Smith MB (1988) Prolonged deterioration of ischemic brain energy metabolism and acidosis associated with hyperglycemia: human cerebral infarction studied by serial ^{31}P NMR spectroscopy. *Ann Neurol* 23:416-418
- Matson GB, Lara RS, Hugg JW, Maudsley AA, Elliott M, Weiner MW (1991) Molar quantitation of ^{31}P metabolites in human brain magnetic resonance spectroscopic imaging. *Proc Soc Magn Reson Med* 10:465
- Maudsley AA, Hilal SK, Perman WH, Simon HE (1983) Spatially resolved high resolution spectroscopy by "four-dimensional" NMR. *J Magn Reson* 51:147-152
- Maudsley AA, Twieg DB, Sappey-Mariniere D, Hubesch B, Hugg JW, Matson GB, Weiner MW (1990) Spin echo ^{31}P spectroscopic imaging in the human brain. *Magn Reson Med* 14:415-422
- Maudsley AA, Lin E, Weiner MW (1992) Spectroscopic imaging display and analysis. *Magn Reson Imag* 10:471-485
- Menon DK, Baudouin CJ, Tomlinson D, Hoyle C (1990) Proton MR spectroscopy and imaging of the brain in AIDS: evidence of neuronal loss in regions that appear normal with imaging. *J Comp Assist Tomogr* 14:882-885
- Nadler JV, Cooper JR (1972) N-Acetyl-L-aspartic acid content of human neural tumours and bovine peripheral nervous tissues. *J Neurochem* 19:313-319
- Nakada T, Houkin K, Hida K, Kwee IL (1991) Rebound alkalosis and persistent lactate: multinuclear (^1H , ^{13}C , ^{31}P) NMR spectroscopic studies in rats. *Magn Reson Med* 18:9-14
- Newsholme P, Newsholme EA (1989) Rates of utilization of glucose, glutamine, and oleate and formation of end-products by mouse peritoneal macrophages in culture. *Biochem J* 261:211-218
- Ordidge RJ, Bendall MR, Gordon RE, Connelly A (1985) Volume selection for in vivo spectroscopy. In: *Magnetic Resonance in Biology and Medicine*. (Govil, Khetrpal, Sarans, eds), New Delhi, Tata-McGraw-Hill, pp 387-397
- Ott D, Ernst T, Hennig J (1990) In vivo ^1H spectroscopy in cerebral ischemia. *Proc Soc Magn Reson Med* 9:1011
- Patt SL, Sykes BD (1972) T₂ water eliminated Fourier transform NMR spectroscopy. *Chem Phys* 56:3182-3184
- Petroff OAC, Prichard JW, Behar KL, Alger JR, den Hollander JA, Shulman RG (1985a) Cerebral intracellular pH by ^{31}P nuclear magnetic resonance spectroscopy *Neurology* 35:781-788
- Petroff OAC, Prichard JW, Behar KL, Rothman DL, Alger JR, Shulman RG (1985b) Cerebral metabolism in hyper- and hypocapnia: ^{31}P and ^1H nuclear magnetic resonance studies. *Neurology* 35:1681-1688
- Petroff OAC, Spencer DD, Alger JR, Prichard JW (1989) High-field proton magnetic resonance spectroscopy of human cerebrum obtained during surgery for epilepsy. *Neurology* 39:1197-1202
- Petroff OAC, Graham GD, Blamire AM, Al-Rayess M, Kim J, Fayad P, Brass LM, Rothman DL, Shulman RG, Prichard JW (1991) ^1H spectroscopic imaging of stroke in man: histopathology correlates of spectral changes. *Proc Soc Magn Reson Med* 10:27
- Plum F (1983) What causes infarction in ischemic brain? The Robert Wartenberg lecture. *Neurology* 33:222-233
- Raichle ME, Posner JB, Plum F (1970) Cerebral blood flow during and after hyperventilation. *Arch Neurol* 23:394-403
- Raley-Susman KM, Cragoe EJ, Jr., Sapolsky RM, Kopito RR (1991) Regulation of intracellular pH in cultured hippocampal neurons by an amiloride-insensitive Na^+/H^+ exchanger. *J Biol Chem* 266:2739-2745
- Rothman DL, Howseman AM, Graham GD, Petroff OAC, Lantos G, Fayad PB, Brass LM, Shulman GI, Shulman RG, Prichard JW (1991) Localized proton NMR observation of $[3-^{13}\text{C}]\text{lactate}$ in stroke after $[1-^{13}\text{C}]\text{glucose}$ infusion. *Magn Reson Med* 21:302-307
- Sappey-Mariniere D, Hubesch B, Matson GB, Weiner MW (1992) Decreased phosphorus metabolites and alkalosis in chronic cerebral infarction. *Radiology* 182:29-34
- Sardet C, Counillon L, Franchi A, Pouyssegur J (1990) Growth factors induce phosphorylation of the Na^+/H^+ antiporter, a glycoprotein of 110 kD. *Science* 247:723-726
- Schuldiner S, Rozengurt E (1982) Na^+/H^+ antiport and Swiss 3T3 cells. Mitogenic stimulation leads to cytoplasmic alkalization. *Proc Natl Acad Sci USA* 79:7778-7782

- Segebarth CM, Balériaux DF, Luyten PR, den Hollander JA (1990) Detection of metabolic heterogeneity of human intracranial tumors in vivo by ^1H NMR spectroscopic imaging. *Magn Reson Med* 13:62-76
- Senda M, Alpert NM, Mackay BC, Buxton RB, Correia JA, Weise SB, Ackerman RH, Doer D, Buonanno FS (1989) Evaluation of the $^{11}\text{CO}_2$ positron emission tomographic method for measuring brain pH. II. Quantitative pH mapping in patients with ischemic cerebrovascular diseases. *J Cereb Blood Flow Metab* 9:859-873
- Siegel GJ, Agranoff BW, Albers RW, Molinoff P (1989) Basic Neurochemistry. New York, Raven Press, p 599
- Syrota A, Samson Y, Boullais C, Wajnberg P, Loc'h C, Crouzel C, Mazière B, Soussaline F, Baron JC (1985) Tomographic mapping of brain intracellular pH and extracellular water space in stroke patients. *J Cereb Blood Flow Metab* 5: 358-368
- Twieg DB, Meyerhoff DJ, Hubesch B, Roth K, Sappey-Marinièr D, Boska MD, Gober J, Schaefer S, Weiner MW (1989) Phosphorus-31 magnetic resonance spectroscopy in humans by spectroscopic imaging: localized spectroscopy and metabolite imaging. *Magn Reson Med* 12:291-305
- Ui M (1966) A role of phosphofructokinase in pH-dependent regulation of glycolysis. *Biochim Biophys Acta* 124:310-322
- Uyeda K (1979) Phosphofructokinase. *Adv Enzymol Relat Areas Mol Biol* 48:193-244
- van Nimmen D, Weyne J, Demeester G, Leusen I (1986) Local cerebral glucose utilization during intracerebral pH changes. *J Cereb Blood Flow Metab* 6:584-598
- van Rijen PC, Luyten PR, Berkelbach van der Sprenkel JW, Kraaier V, van Huffelen AC, Tulleken CAF, den Hollander JA (1989) ^1H and ^{31}P NMR measurement of cerebral lactate, high-energy phosphate levels, and pH during voluntary hyperventilation: associated EEG, capnographic, and doppler findings. *Magn Reson Med* 10:182-193
- Vigneron DB, Nelson SJ, Murphy-Boesch J, Kelley DAC, Kessler HB, Brown TR, Taylor JS (1990) Chemical shift imaging of human brain: axial, sagittal, and coronal P-31 metabolite images. *Radiology* 177:643-649
- Weiner MW, Hetherington HP, Hubesch B, Karczmar G, Massie B, Maudsley AA, Meyerhoff DJ, Sappey-Marinièr D, Schaefer S, Twieg DB, Matson GB (1989) Clinical magnetic resonance spectroscopy of brain, heart, liver, kidney, and cancer: a quantitative approach. *NMR Biomed* 2: 290-297
- Welch KMA, Helpert JA, Robertson WM, Ewing JR (1985) ^{31}P topical magnetic resonance measurement of high energy phosphates in normal and infarcted brain. *Stroke* 16:151-157